

The effect of pressure and spin on the isotopic composition of ferrous iron dissolved in periclase and silicate perovskite

James R. Rustad, Piotr Zarzycki, Maryali P. Saucedo, and Qing-zhu Yin

*Department of Geology, University of California-Davis,
One Shields Avenue, Davis, CA 95616 U. S. A.**

(Dated: November 9, 2021)

We perform density functional calculations of the equilibrium $^{57}\text{Fe}/^{54}\text{Fe}$ ratios for ferrous iron dissolved in periclase and MgSiO_3 perovskite at the pressures and temperatures of the Earth's mantle. Pressure increases the partitioning of ^{57}Fe into both phases by a factor of three from the Earth's surface to the core-mantle boundary. In ferropericlase, a large contribution to this increase comes from the electronic transition from high-spin to low-spin iron. Our calculations demonstrate that pressure-induced fractionation can play a major role in determining planetary iron-isotope composition.

PACS numbers: 62.50.-p,91.35.Gf,71.15.Mb,91.65.-n,91.65.Dt

The distribution of iron-isotopes between and within planetary bodies provides constraints on their histories of accretion and differentiation [1, 2, 3]. A significant fraction of the iron in the silicate Earth is dissolved in periclase ($\text{Fe}_x\text{Mg}_{1-x}\text{O}$) (**fep**) and silicate perovskite ($\text{Fe}_x\text{Mg}_{1-x}\text{SiO}_3$) (**fepv**) which make up the bulk of the Earth's lower mantle [4]. Uptake by **fep** and **fepv** has almost certainly influenced the distribution of iron-isotopes in the Earth, but little is known definitively about the equilibrium iron isotope compositions of these phases at lower-mantle pressures and temperatures. Empirical estimates, based on the vibrational density of states for the iron-sublattice obtained from Mössbauer spectroscopy and inelastic nuclear resonant X-ray scattering (INRXS) techniques, are starting to address this issue [5, 6].

Equilibrium isotopic signatures should become heavier with increasing pressure as bonds are compressed and vibrational frequencies increase. Because the ionic radius of low-spin iron is smaller than high-spin iron, iron-isotope signatures also may be made heavier by the spin transition for Fe^{2+} [7, 8], which, in **fep**, is predicted to occur within the Earth's mantle [9, 10]. The reduced partition function ratio (β), can be used to make predictions of the effect of pressure and electronic state on the possible isotopic fractionations associated with **fep** and **fepv**. In the harmonic approximation β is defined by [11]:

$$\beta = \left(\frac{Q_h}{Q_l} \right) = \prod_i \frac{e^{-u_{hi}/2}}{1 - e^{-u_{hi}}} \frac{1 - e^{-u_{li}}}{e^{-u_{li}/2}} \quad (1)$$

where $u_{(h,l)_i} = \hbar c 2\pi \omega_{(h,l)_i} / kT$, h and l refer to the heavy isotope and light isotope, respectively (here ^{57}Fe and ^{54}Fe), T is the temperature, and the product runs over all frequencies ω_i . The equilibrium constant for isotopic exchange α between phases i and j is given as $\alpha_{i,j} = \beta_i / \beta_j$; $\alpha_{i,j} > 1$ implies that the heavy isotope is concentrated in phase i . Here we use density functional electronic structure methods to calculate β for Fe^{2+} in **fepv** and **fep** at

pressures and temperatures near that of the core-mantle boundary. We have found that β increases dramatically with pressure and is strongly affected by the high-spin to low-spin transition in **fep**.

Density functional calculations have made important contributions to understanding the properties of lower mantle phases [8, 10, 12]. They also have been used to estimate isotope fractionation factors in iron-bearing phases such as $\text{Fe}^{2+,3+}(\text{aq})$ via harmonic vibrational frequencies [13, 14]. Here, we use these methods on clusters representative of the coordination environment of Fe^{2+} in **fep** and **fepv**. The clusters can be treated with standard all-electron quantum chemistry methods, avoiding potential problems of the iron pseudopotential and making a stronger connection with existing studies of vibrational frequencies and the spin-crossover transition in the quantum chemistry literature, which can guide the choice of exchange-correlation functionals and basis set [15]. Such methods allow affordable use of hybrid exchange-correlation functionals which can make accurate estimates of the spin-crossover energies in extensive studies on molecular systems [16] and have provided the best estimates of isotope fractionation factors [17]. The hybrid functionals complement calculations using the local-density and generalized-gradient approximations [8, 12] and studies using the Hubbard model [10].

Iron atoms are assumed to vibrate in coordination environments characteristic of **fep** and **fepv**, similar to the site-specific vibrational density of states approach adopted in Ref. [6]. The models consist of a free "core" surrounded by a rigid shell of oxygen atoms fixed in their ideal lattice positions. The vibrational modes of the core within the cavity that displace the iron center are assumed to approximate the vibrational modes that govern equilibrium isotopic fractionation in the crystal. The cores of the clusters are shown in Figure 1. The **fepv** site consists of a single iron atom and eight coordinating oxide atoms. All silicon and magnesium atoms attached to these eight oxygens are also included in the core cluster. The core is surrounded by a layer of oxygen atoms completing the coordination shells of the silicon and mag-

*Electronic address: jrrustad@ucdavis.edu

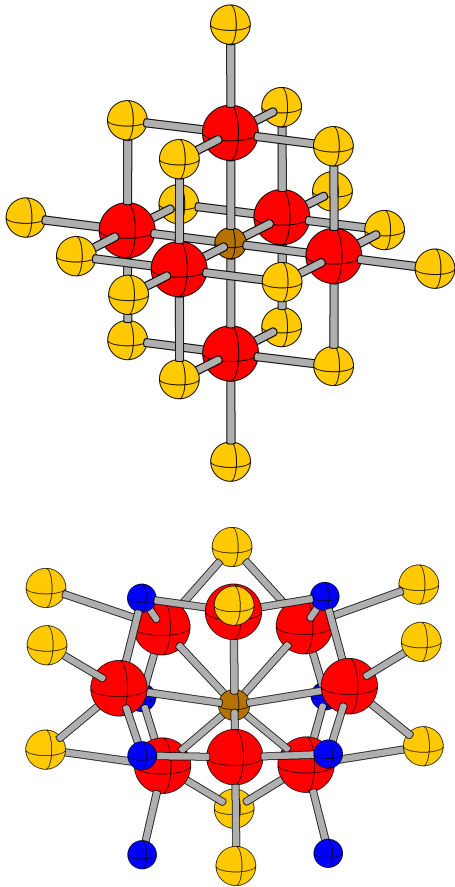


FIG. 1: Core atoms of molecular clusters used to model periclase (**fep**, above) and fe-perovskite (**fepv**, below). The iron atom (brown) is centered within its coordination environment of oxygen (red), magnesium (yellow) and silicon (blue). These core atoms are fully relaxed within a shell of oxygen atoms, fixed in their ideal lattice positions. This rigid outer shell of oxygen atoms is capped by hydrogen atoms having fractional charges as described in the text.

nesium atoms. The other bonds into the outer layer of oxygen atoms coming from “external” magnesium and silicon atoms, are represented by link atoms having a charge equal to the Pauling bond strength (the charge divided by the coordination number) contributed into the oxygen atom. The link atoms are placed along the broken bonds one ångström away from the oxygen atom. This procedure ensures a neutral, auto-compensated cluster. The **fep** cluster, centered on the octahedral iron site, is constructed in the same manner. This simple technique accurately reproduces calculations of isotope fractionation in carbonates and other oxide minerals with periodic boundary conditions [17, 18].

The electronic structure calculations, carried out with the PQS quantum chemistry package of Pulay, Baker, and co-workers (<http://www.pqs-chem.com>). The rigid

TABLE I: Calculated bond lengths, in Å, with multiplicities given in parentheses, if different from unity.

fepv		fep			
high-spin		high-spin		low-spin	
0	120	0	120	0	120
1.958	1.857	2.213 (2)	1.978 (2)	2.213 (6)	1.959 (6)
2.149	1.927	2.276 (4)	2.008 (4)		
2.034 (2)	1.866 (2)				
2.462 (2)	2.062 (2)				
2.478 (2)	2.212 (2)				

outer shell uses the 3-21G basis on both the oxygen atoms and the link atoms (which use hydrogen basis functions). The optimized atoms use the 6-31G* basis for O, Mg, and Si, and the *m*6-31G* basis for Fe [19]. The B3LYP exchange-correlation functional, as implemented in the PQS code, was used for the exchange-correlation functional. For **fepv** outer-shell oxygen positions were taken from Ref. [20] at 0 GPa and from electronic structure calculations [21] at 120 GPa. Lattice parameters for **fep** were obtained from a recent universal P-V-T equation of state for periclase [22]. The high-pressure lattice parameters were taken at 120 GPa and at the highest available temperature of 3000 K, even though we evaluate Eq. 1 at 4000 K. The low-pressure lattice parameters were taken at 0 GPa and 300 K.

For the **fepv** cluster, we enforce mirror symmetry through the center of the cluster perpendicular to the **c** crystallographic axes, giving the cluster point symmetry C_s . For the low-spin **fep** cluster we retain the T_h symmetry group; this is relaxed in the high-spin cluster which was run with no symmetry constraints to accommodate possible Jahn-Teller distortions. The positions of the central iron atom, its coordinating oxygen atoms, and the magnesium and silicon atoms attached to the coordinating oxygen atoms are optimized within the rigid outer shell of the cluster (oxygen atoms and link atoms). Relaxed bond lengths in the primary coordination sphere of the iron for all clusters are given in Table 1.

The Hessian matrix for the free atoms was calculated analytically by projecting out the degrees of freedom of the fixed atoms. Harmonic vibrational frequencies were calculated for the core atoms with both ^{54}Fe and ^{57}Fe , and used to estimate β in the harmonic approximation according to Eq. 1. The β defined by Eq. 1 was divided by the high temperature limiting value β_{HT} according to standard convention [23].

Calculations on low-spin Fe^{2+} in the **fepv** cage in C_s symmetry gave a vibrational mode with an imaginary frequency perpendicular to the mirror plane. low-spin Fe^{2+} would therefore “rattle” unfavorably in a cage with C_s symmetry, qualitatively consistent with the idea the Fe^{2+} is not likely to undergo a pressure-induced high-spin to low-spin transition in **fepv** in the Earth’s mantle [24]. We did not consider low-spin Fe^{2+} further in the **fepv** cluster. Fe^{3+} in the octahedral Si^{4+} site may un-

TABLE II: Reduced partition function ratios $10^3 \ln(\beta/\beta_{HT})$, calculated for ^{57}Fe and ^{54}Fe , according to Eq. 1 and as described in the text.

P (GPa)	fepv		fep			
	high-spin		high-spin		low-spin	
300 K	9.86	24.2	7.04 (7.8) ^a	16.5	8.1	24.1 (20.1) ^{ab}
4000 K ^c	0.06	0.15	0.04	0.10	0.05	0.15

^ataken from Ref. 6

^bP = 109 GPa

^cthe periclase lattice parameters are taken at 120 GPa and 3000 K from Ref. 22, but the β was evaluated at 4000 K in Eq. 1

dergo spin crossover within the mantle [12], but this is not considered here.

The results of the calculations are shown in Table 2, given as $10^3 \ln(\beta/\beta_{HT})$, for temperatures of 300 K and 4000 K, the latter temperature being close to that of the core-mantle boundary. First, pressures at the core-mantle boundary increase the β factors for both phases by a factor of 2.5-3 relative to the Earth's surface. For **fep** at pressures near the core-mantle boundary, half of the enrichment can be attributed to the high-spin to low-spin transition in **fep**. A much smaller difference is predicted at ambient pressures. Although we do not claim to be able to quantitatively model the energetics of the spin transition here, we remark that the electronic energy for the cluster with low-spin iron **fep** is approximately 1.5 eV above that for the cluster with high-spin iron at 0 GPa. In the high-pressure cluster, however, the electronic energy of the low-spin cluster is about 0.4 eV *below* that for high-spin cluster. The β values for **fep** given in Table 2 are in reasonable agreement with those reported in [6]. The high-pressure value of β is somewhat lower than our calculations. Part of the reason for this is that the high-pressure value of β based on INRXS measurements is given at 109 GPa whereas the calculations were carried out at ≈ 120 GPa.

The contributions to β for the high-spin and low-spin **fep** clusters are shown in Fig. 2. Contributions to β are spread out among seven main fractionating modes. Characteristic motions associated with these modes are given in Fig. 3. For both the high-spin and low-spin configurations, the largest contribution to β comes from the fundamental vibration of the central iron against the cage of surrounding oxygens and magnesium ions at 308 (302) cm^{-1} for ^{54}Fe (^{57}Fe) in low-spin **fep**. This is an acoustic mode with the coordinating oxygen atoms and magnesium atoms moving with the iron, but with less displacement. Although this mode makes the biggest contribution to β , the difference between the high-spin and low-spin contributions is not very large. The next most important fractionating mode is at 491.3 (489.80) cm^{-1} , an optical mode involving the iron atom vibrating against its own foxygen coordination shell and their attached magnesium atoms. In the high-spin **fep** clus-

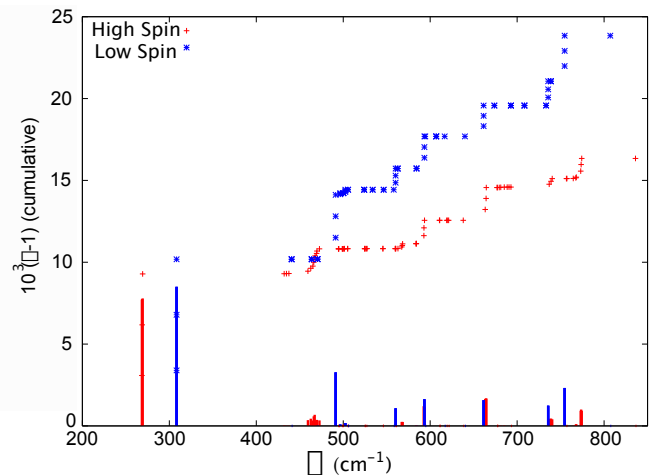


FIG. 2: Cumulative value of $(\beta-1)$ for high-spin and low-spin **fep** cluster at $P \approx 120$ GPa. Contributions of different vibrational modes to β are given by impulses.

ter, this mode occurs at somewhat lower frequencies, and is spread out among several similar modes. This mode does not fractionate iron as intensely in the high-spin cluster as it does in the low-spin cluster; β is nearly four per mil lower than the low-spin cluster after passing through these vibrational modes. The mode at 560.3 (559.8) cm^{-1} in the low-spin cluster, mostly involving motion of the equatorial FeO_4 plane against the oxygens at the apex, also makes a much larger contribution to β than the corresponding vibration in the high-spin cluster. The next two vibrational modes make roughly equal contributions to β in both the high- and low-spin clusters. The last two modes, involving primary stretching of the FeO_6 octahedron, with the iron in phase with the magnesium atoms, again make stronger contributions for the low-spin cluster than for the high-spin cluster.

The magnitudes of the increases in β with pressure has implications for the isotopic signatures of accreting planetary bodies. First, an individual planet in isotopic equilibrium should be isotopically stratified with heavier isotopes progressively concentrated at depth within the planet. Such a stratification could possibly be established during a “magma ocean” stage as iron isotopes sample coordination environments in liquid silicates that would be similar to **fep** or **fepv**. An interesting question is whether a spin transition would take place in the melt. If coordination environments are structurally closer to **fepv** [25], the spin transition may be suppressed and the isotopic signature could be lighter than a solid of the same composition. Freezing of a magma ocean might be expected to give rise to an isotopically stratified mantle with the heavy isotopes accumulating preferentially at the base, depending on the relative densities of the liquid and solid phases.

If an equilibrium isotopic profile, with $^{57}\text{Fe}/^{54}\text{Fe}$ increasing with depth, can be established after impact events, evaporative loss of surface material during ex-

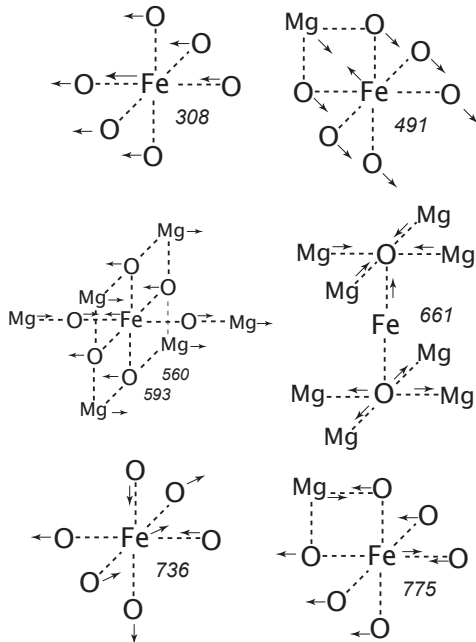


FIG. 3: Major fractionating vibrational modes shown in Fig. 2. Numbers in italics give vibrational frequencies in cm^{-1} . The modes at 560 cm^{-1} and 593 cm^{-1} involve similar displacements of the central iron atom.

tre heating would be isotopically light, thus the larger planets should be isotopically heavier than the smaller planets, because the larger planets can shield greater reservoirs of material at high-pressure where the β factor is larger. This may be part of the reason why the Earth-Moon system appears to be isotopically heavier than Mars and Vesta [26].

The pressure dependence of β is sensitive to crystallographic environment; β_{fepv} increases more than a factor of two over high-spin β_{fep} , probably because of the greater compressibility of the coordination shell in **fepv**. However, the increase is compensated completely at the core-mantle boundary by the spin transition in **fep**. The similarity between β_{fepv} and β_{fep} indicates little differential isotopic fractionation between these phases after the spin-transition takes place in the lower mantle. Above this transition, we expect **fepv** to be enriched in ^{57}Fe over **fep** by a factor of two.

Acknowledgments

This work was funded by the U. S. Department of Energy, division of Basic Energy Sciences, grant DE-FG02-04ER15498, and NSF grant EAR-08-14242.

-
- [1] B. L. Beard and C. M. Johnson, *Geochim. Cosmochim. Acta* **68**, 4727 (2004).
 - [2] S. Weyer, A. D. Anbar, G. P. Brey, C. Munker, K. Mezger, and A. Woodland, *Earth and Planet. Sci. Lett.* **240**, 251 (2005).
 - [3] F. Poitrasson, *Earth and Planet. Sci. Lett.* **256**, 484 (2007).
 - [4] S. E. Kesson, J. D. FitzGerald, and J. M. Shelley, *Nature* **393**, 252 (1998).
 - [5] V. B. Polyakov, R. N. Clayton, J. Horita, and S. D. Mineev, *Geochim. Cosmochim. Acta* **71**, 3833 (2007).
 - [6] V. B. Polyakov, *Geophysical Research Abstracts* **10**, 10347 (2008).
 - [7] W. S. Fyfe, *Geochim. Cosmochim. Acta* **19**, 141 (1960).
 - [8] R. E. Cohen, I. I. Mazin, and D. G. Isaak, *Science* **275**, 654 (1997).
 - [9] S. Speziale, A. Milner, V. E. Lee, S. M. Clark, M. P. Pasternak, and R. Jeanloz, *Proc. Nat. Acad. Sci.* **102**, 17918 (2005).
 - [10] T. Tsuchiya, R. M. Wentzcovitch, C. R. S. da Silva, and S. de Gironcoli, *Phys. Rev. Lett.* **96**, 198501 (2006).
 - [11] J. Bigeleisen and M. G. Mayer, *J. Chem. Phys.* **15**, 261 (1947).
 - [12] S. Stackhouse, J. Brodholt, and G. Price, *Earth and Planet. Sci. Lett.* **253**, 282 (2007).
 - [13] P. S. Hill and E. A. Schauble, *Geochim. Cosmochim. Acta* **72**, 1939 (2008).
 - [14] A. D. Anbar, A. A. Jarzecki, and T. G. Spiro, *Geochim. Cosmochim. Acta* **69**, 825 (2005).
 - [15] S. Zein, S. A. Borshch, P. Fleurat-Lessard, M. Casida, and H. Chermette, *J. Chem. Phys.* **126**, 014105 (2007).
 - [16] A. Fouqueau, S. Mer, M. E. Casida, L. M. L. Daku, A. Hauser, T. Mineva, and F. Neese, *J. Chem. Phys.* **120**, 9473 (2004).
 - [17] J. R. Rustad, S. L. Nelmes, V. E. Jackson, and D. A. Dixon, *J. Phys. Chem. A* **112**, 542 (2008).
 - [18] J. R. Rustad and P. Zarzycki, *Proc. Nat. Acad. Sci.* **105**, 10297 (2008).
 - [19] A. V. Mitin, J. Baker, and P. Pulay, *J. Chem. Phys.* **118**, 7775 (2003).
 - [20] C. B. Vanpeteghem, R. J. Angel, N. L. Ross, S. D. Jacobsen, D. P. Dobson, K. D. Litasov, and E. Ohtani, *Physics of the Earth and Planetary Interiors* **155**, 96 (2006).
 - [21] T. Itaka, K. Hirose, K. K. K., and M. Murakami, *Nature* **430**, 442 (2004).
 - [22] J. Garai, J. Chen, H. Couvy, and G. Telekes, *physics.geoph* **1**, 1 (2008).
 - [23] T. Chacko, T. K. Mayeda, R. N. Clayton, and J. R. Goldsmith, *Geochim. Cosmochim. Acta* **55**, 2867 (1991).
 - [24] A. M. Hofmeister, *Earth Planet. Sci. Lett.* **243**, 44 (2006).
 - [25] L. Stixrude and B. Karki, *Science* **310**, 297 (2005).
 - [26] F. Poitrasson, *Earth and Planet. Sci. Lett.* **223**, 253 (2004).